Organic & Biomolecular Chemistry

PAPER

View Article Online
View Journal | View Issue

Cite this: *Org. Biomol. Chem.*, 2014, **12**, 4163

Quantum mechanistic insights on aryl propargyl ether Claisen rearrangement†

Venkatesan Srinivasadesikan,[a] Jiun-Kuang Dai[b] and Shyi-Long Lee*[b]

Received 19th February 2014,
Accepted 25th March 2014

DOI: 10.1039/c4ob00388h

www.rsc.org/obc

The mechanism of aryl propargyl ether Claisen rearrangement in gas and solvent phase was investigated using DFT methods. Solvent phase calculations are carried out using *N*,*N*-diethylaniline as a solvent in the PCM model. The most favorable pathways involve a [3,3]-sigmatropic reaction followed by proton transfer in the first two steps and then deprotonation or [1,5]-sigmatropic reaction. Finally, cyclization yields benzopyran or benzofuran derivatives. The [3,3]-sigmatropic reaction is the rate-determining step for benzopyran and benzofuran with $\Delta G^{\ddagger}$ value of 38.4 and 37.9 kcal mol^{-1} at M06/6-31+G**//B3LYP/6-31+G* level in gas and solvent phase, respectively. The computed results are in good agreement with the experimental results. Moreover, it is found that the derivatives of aryl propargyl ether proceeded Claisen rearrangement and the rate-determining step may be shifted from the [3,3]-sigmatropic reaction to the tautomerization step. The NBO analysis revealed that substitution of the methyl groups on the aliphatic segment has decreased the stabilization energy *E*(2) and favors the aryl propargyl ether Claisen rearrangement.

1. Introduction

The Claisen rearrangement is a versatile tool in organic synthesis to form a carbon–carbon bond[1] and the first recorded example of a [3,3]-sigmatropic reaction.[2] Since it was discovered in 1912, this reaction has continued to be advanced in methods or in applications towards the total synthesis of natural products and pharmacologically relevant molecules. The benzofuran and benzopyran derivatives are ubiquitous in nature and also serve as versatile synthetic intermediates in pharmaceuticals. Those compounds can be obtained easily by aryl propargyl ether Claisen rearrangement[3] and the mechanism has been speculated by Zsindely and Schmidt.[4] However, few experimental reports on the aryl propargyl ether Claisen rearrangement have been reported[3–10] and there is need of quantum mechanical calculations to support the mechanistic speculation. In this paper, detailed quantum mechanical calculations were carried out and presented for all plausible mechanisms.

There are a number of approaches for the synthesis of benzofuran and/or benzopyran.[11–24] However, most of the methods suffer from one or more disadvantages including low yield, toxicity and cost of reagents, long reaction time and environmental pollutions, *etc*. In addition, some of these approaches are lack of flexibility in terms of substituents. Otherwise, a simple route was reported by Iwai and Ide which was established for rearrangement of simple aryl propargyl ether in *N*,*N*-diethylaniline at higher temperature and yielded benzopyrans[3] but the yield was not ideal. Moreover, the substituent effect of aryl propargyl ether was also discussed to increase the yield.[5–9] After a number of detailed examinations of aryl propargyl ether Claisen rearrangement, a route in presence of cesium fluoride (CsF) leading to formation of 2-methylbenzofuran in excellent yield was reported by Ishii *et al.*[10] Therefore, the thermal rearrangement of aryl propargyl ether leads to an effective and convenient procedure for yielding benzopyran or benzofuran. Lingam *et al.* also explained that the rearrangement has highly functionalized properties.[19] However, when the *meta*-substituent aryl propargyl ether proceeded *via* the Claisen rearrangement, it has been observed that two orientations can be carried out to yield two different products that we denoted as *ortho*- and *para*-cyclized product with regioselectivity. Anderson *et al.* have attempted to provide reasonable explanation for regioselectivity.[8,9] Unfortunately, this is difficult without knowing which step is the rate-determining step that affects the substituent effects and then influences the final yield. Therefore, it is important to realize the complete mechanism of aryl propargyl ether Claisen rearrangement.

Since 1984, the Claisen rearrangement has been studied theoretically,[25] which used MNDO to analyze the transition

[a]*Department of Applied Chemistry, National Chiao Tung University, Hsinchu, Taiwan*
[b]*Department of Chemistry and Biochemistry, National Chung Cheng University, Taiwan. E-mail: chesll@ccu.edu.tw*

†Electronic supplementary information (ESI) available. See DOI: 10.1039/c4ob00388h

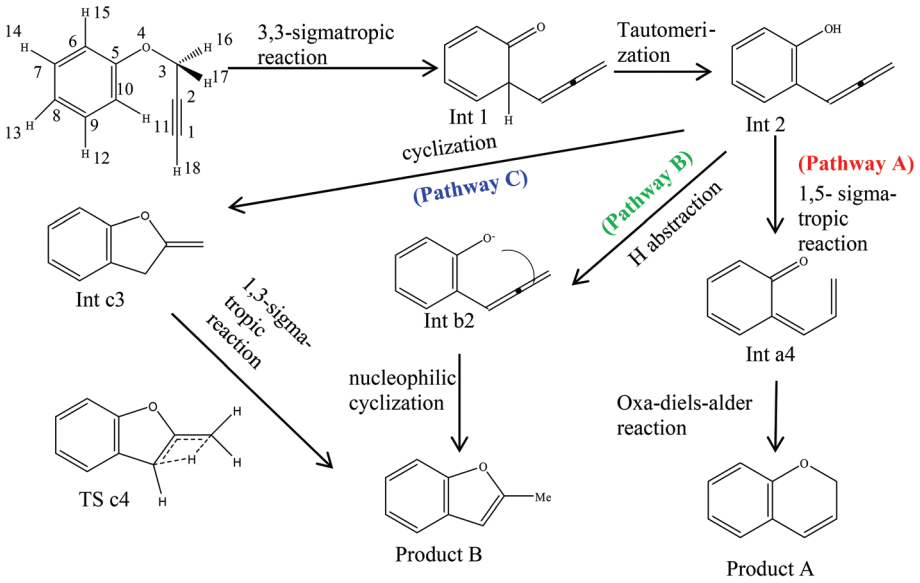

Scheme 1 Schematic representation of the mechanism for the formation of benzopyran and 2-methylbenzofuran in aryl propargyl ether Claisen rearrangement.

state structures. Since then, a number of Claisen rearrangements have been reported by semi-empirical, *ab initio* and DFT computational studies. However, most of the studies concentrated on allyl vinyl ethers and aryl vinyl ethers. The computational reports on Claisen rearrangement were, *e.g.*, Ireland-Claisen rearrangement for the effects of substituents on the transition state and for stereoselectivity,[26,27] Gosteli–Claisen rearrangement for describing the substituent rate effect quantitatively[28] and "on water" reaction to know the reactivity for aromatic Claisen rearrangement by QM/MM methods.[29,30] However, there is lack of theoretical aryl propargyl ether Claisen rearrangement and the reaction is important for the synthesis of benzopyran or benzofuran. Moreover, the rate-determine step is also uncertain. Therefore, in the present work we set out to obtain plausible mechanistic pathways and also to recognize the rate-determining step by state-of-the-art quantum mechanical methods.

In this article, the reaction pathways in Scheme 1 are examined and then the rate-determining step is determined from the potential energy surface (PES) by DFT calculations. Moreover, the rate constant of the reactions has also been calculated to examine which method is suitable to describe the systems. The rationalized discussion has also been presented for the product of benzopyran and benzofuran from aryl propargyl ether using the potential energy surface. Subsequently, the substituent effects, NBO analysis and pK_a results have been discussed.

2. Computational methods

2.1. Computational methods

Geometry optimizations have been performed at B3LYP[31–35] with the basis set 6-31+G*. The same level of method was used for the frequency calculations at all the optimized structures. Zero point vibrational energy (ZPVE) corrections are included in the total energy. The intrinsic reaction coordinate (IRC) calculations have also been carried out to verify the identity of the transition state (TS) structures and to obtain the potential energy surface profile connecting the TS to the two associated minima of the proposed mechanisms. Single-point energy calculation is performed by different DFT methods (M06-2X,[36] M05-2X,[37] M06,[36] M05,[38] ωB97XD,[39] BMK,[40] B2PLYP[41]) with the basis set of 6-31+G**. The solvation energies are computed using *N*,*N*-diethylaniline (ε = 5.5) as a solvent with self-consistent reaction field (SCRF) method using the polarized continuum model (PCM).[42,43] All calculations have been performed with the Gaussian 09 package.[44]

Natural bond orbital (NBO)[45,46] analysis are performed at M06/6-31+G**//B3LYP/6-31+G* level using NBO 3.0 version included in Gaussian 09 package. All possible interactions were between filled (donor) Lewis type and empty (acceptor) non-Lewis type NBOs, and their energies were estimated by 2nd-order perturbation theory. For each donor NBO (i) and acceptor NBO (j), the stabilization energy $E(2)$ associated with delocalization $i \rightarrow j$ is estimated as

$$E(2) = \Delta E_{ij} = q_i \frac{(F(i,j))^2}{\varepsilon_j - \varepsilon_i}$$

where q_i is the donor orbital occupancy, ε_j, ε_i are diagonal elements (orbital energies) and $F(i,j)$ is the off-diagonal NBO Fock matrix element. The larger $E(2)$ value indicates that the interaction between donor and acceptor is stronger.

2.2. Comparison of different DFT methods

A benchmark study has been carried out for aryl propargyl ether Claisen rearrangement in order to evaluate the DFT

Table 1 Relative Gibbs free energy of the aryl propargyl ether Claisen rearrangement at M06/6-31+G**//B3LYP/6-31+G* level (unit: kcal mol^{-1})

	M06/6-31+G**//B3LYP/6-31+G*	
	Gas	Solvent
Reactant	0.0	0.0
TS1	38.4	37.9
Int1	4.3	3.0
TS2-1	52.6	52.1
TS2-2	34.0	33.6
Int2	−20.5	−21.1
TSa3	5.1	4.1
Inta3	−20.2	−21.8
Tsa4	−10.0	−11.1
Inta4	−14.8	−16.6
TSa5	−3.9	−5.1
Product A	−36.4	−37.1
Intb2	321.4	185.9
TSb3	336.1	202.7
Product B cpx	304.0	183.3
TSc3	49.9	49.7
Intc3	−37.3	−37.3
TSc4	30.6	29.9
Product B	−51.3	−51.1

methods on the activation energy. Our computed activation energies can be compared with the experimental rate constants.[7] Recently, Ramadhar *et al.* has also reported a benchmark study to evaluate the performance of different DFT methods on the activation barrier ($\Delta G^{\ddagger}$) for aliphatic-Claisen rearrangement and indicated that single point energies computed by M05, M06 and M08 functionals on B3LYP optimized structures could give better estimated values.[47] Optimization as well as frequency analysis are carried out at B3LYP/6-31+G* level, then the single-point energies are computed by different DFT methods (B3LYP, M06-2X, M06, M05-2X, M05, wB97XD, BMK and B2PLYP) with the basis set of 6-31+G** in the solvent-phase. The calculated results are shown in Table 2.

As seen in Table 2, M06 and M05 methods provide better results with the root mean square error (RMSE) of 1.4 kcal mol^{-1} and 1.2 kcal mol^{-1}, respectively, and mean unsigned error (MUE) of 1.0 kcal mol^{-1} and 1.1 kcal mol^{-1}, respectively. The M06 functional is selected to further examine the basis set effects. The results of M06 with different basis set size are shown in Table 3. As seen in Table 3, while increasing the basis set size the RMSE and MUE values decrease slightly and level out at 6-31+G** for M06 functional. It suggests that a more flexible basis set than 6-31+G** may not be beneficial to prediction of the energy barriers for aryl propargyl ether Claisen rearrangement. Based on the aforementioned analysis, the M06/6-31+G**//B3LYP/6-31+G* level has the best performance for the eleven aryl propargyl ether Claisen rearrangement reaction barriers with a precision of 1.3 and 0.9 kcal mol^{-1} for RMSE and MUE, respectively. Therefore, the M06/6-31+G**//B3LYP/6-31+G* level is adopted in our further analysis for aryl propargyl ether Claisen rearrangement.

3. Results and discussion

3.1. Mechanism and structures

The plausible mechanism of aryl propargyl ether Claisen rearrangement is described in Scheme 1 and the selected geometries in the gas phase are shown in Fig. 1. As shown in Scheme 1, step 1 belongs to Claisen rearrangement with a cyclic transition state (TS 1 in Fig. 1). This is a reaction with a σ bond which migrates from one end of a π system to the other, that is, the breaking of C3–O4 bond and forming C1–C10 bond. In the proton transfer step (Step 2), there are two possible pathways: intramolecular or intermolecular proton

Table 2 Theoretical activation free energies of aryl propargyl ether Claisen rearrangement at B3LYP/6-31+G* level optimization geometries and different DFT methods with the basis set 6-31+G* for single point energy in *N*,*N*-diethylaniline (unit: kcal mol^{-1})

						$\Delta G^{\ddagger}$(calc.)[e]							
	R1	R2	X	$k \times 10^6$, s^{-1} at 161.6 °C	$\Delta G^{\ddagger}$(exp.)[d]	B3LYP	M06-2X	M06	M05-2X	M05	wB97XD	BMK	B2PLYP
1	H	H	H	0.962	37.8	34.9	41.8	37.6	39.7	38.5	39.7	40.0	34.5
2	H	H	Cl	0.722	38.2	35.1	42.3	37.8	40.3	38.9	40.1	40.6	34.6
3	H	H	NO_2	0.252	38.9	36.2	43.5	38.9	41.7	40.2	41.2	42.0	36.1
4	H	H	OCH_3	1.15	37.6	34.8	42.8	37.8	40.8	38.8	40.3	40.8	34.4
5	CH_3	H	H	3.49	36.6	33.4	41.0	35.5	39.3	37.1	38.5	39.8	33.4
6	CH_3	H	Cl	3.79	36.5	33.6	41.5	35.8	39.9	37.3	38.9	40.0	33.7
7	CH_3	H	NO_2	2.27	37.0	33.9	42.2	35.9	40.7	37.5	39.4	40.6	34.6
8	CH_3	H	OCH_3	9.98	35.8	33.4	42.0	35.7	40.3	37.2	39.2	40.2	33.5
9	CH_3	CH_3	H	203	33.1	27.6	36.9	30.5	35.3	31.3	34.1	35.1	28.4
10	CH_3	CH_3	NO_2	350	32.7	27.2	37.2	29.7	35.9	30.5	34.1	35.0	29.1
11	CH_3	CH_3	OCH_3	628	32.2	27.5	38.0	30.8	36.7	31.0	35.1	35.3	28.6
					R[a]	0.9861	0.9463	0.9825	0.9252	0.9847	0.9663	0.9627	0.9776
					RMSE[b]	3.7	4.9	1.4	3.2	1.2	2.3	3.1	3.3
					MUE[c]	3.5	4.8	1.0	3.1	1.1	2.2	3.0	3.2
					Max. abs. error	5.5	6.2	3.0	4.5	2.2	3.4	4.4	4.7

[a] R = Pearson correlation coefficient. [b] RMSE = root-mean-square error. [c] MUE = mean unsigned error. [d] Exp.: experimental values. [e] Calc. = calculated.

Table 3 Theoretical activation free energies of aryl propargyl ether Claisen rearrangement at B3LYP/6-31+G* level optimization geometries and M06 single point energy calculation with different basis sets in *N*,*N*-diethylaniline (unit: kcal mol^{-1})

						M06					
						$\Delta G^{\ddagger}$(calc.)[e]					
	R1	R2	X	$k \times 10^6$, s^{-1} at 161.6 °C	$\Delta G^{\ddagger}$(exp.)[d]	6-31+G*	6-31+G**	6-31++G*	6-311++G**	6-311++G(2d,p)	6-311++G(2d,2p)
1	H	H	H	0.962	37.8	37.6	37.6	37.5	38.9	38.9	38.9
2	H	H	Cl	0.722	38.2	37.8	37.8	37.8	38.9	39.0	39.1
3	H	H	NO_2	0.252	38.9	38.9	38.9	38.8	39.7	39.9	40.0
4	H	H	OCH_3	1.15	37.6	37.8	37.8	37.7	38.8	38.9	39.0
5	CH_3	H	H	3.49	36.6	35.5	35.6	35.4	36.4	36.7	36.8
6	CH_3	H	Cl	3.79	36.5	35.8	35.8	35.7	36.6	36.9	37.0
7	CH_3	H	NO_2	2.27	37.0	35.9	36.0	35.9	36.5	37.0	37.1
8	CH_3	H	OCH_3	9.98	35.8	35.7	35.8	35.7	36.6	36.9	37.0
9	CH_3	CH_3	H	203	33.1	30.6	30.7	30.7	31.1	31.5	31.6
10	CH_3	CH_3	NO_2	350	32.7	29.7	29.9	29.6	30.2	30.7	30.8
11	CH_3	CH_3	OCH_3	628	32.2	34.8	33.3	34.9	34.8	34.7	35.1
					R[a]	0.8662	0.9330	0.8585	0.8977	0.9161	0.9041
					RMSE[b]	1.5	1.3	1.5	1.4	1.3	1.4
					MUE[c]	1.1	0.9	1.1	1.1	1.1	1.2
					Max. abs. error	3.0	2.8	3.1	2.6	2.5	2.9

[a] R = Pearson correlation coefficient. [b] RMSE = root-mean-square error. [c] MUE[c] = mean unsigned error. [d] Exp.: experimental values. [e] Calc. = calculated.

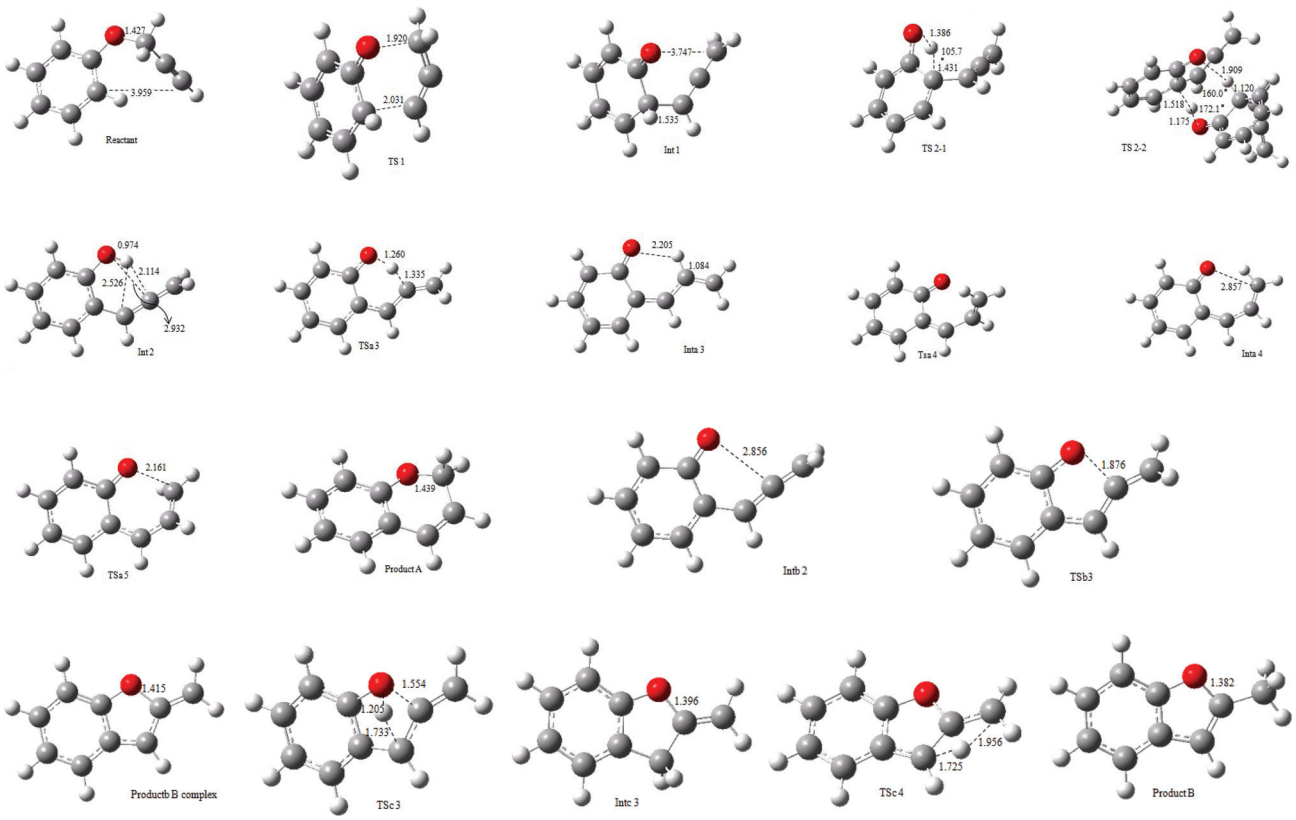

Fig. 1 Optimized geometries at B3LYP/6-31+G* level in the gas phase (bond lengths in Å and bond angles in °).

transfer as proposed in the previous literature.[30,48] The calculated results of Yamabe *et al.* indicate that intermolecular proton transfer has a more reliable mechanism than intramolecular proton transfer in the second step of the aromatic Claisen rearrangement.[48] Our results also favor intermolecular proton transfer (TS2-2) which is in good agreement with the

previous report. Three possible mechanisms are then followed from Int2: one is [1,5]-sigmatropic reaction followed by isomerization to form benzopyran *via* cyclization, another is H abstraction followed by cyclization to 2-methylbenzofuran and the third one is cyclization followed by [1,3]-sigmatropic reaction to 2-methylbenzofuran.

As shown in Fig. 1, in the first step, the C3–O4 bond length is elongated from 1.427 Å in the reactant to 1.920 Å in TS1 and further to 3.747 Å in Int1. Meanwhile, the C1–C10 bond length is shortened from 3.959 Å in the reactant to 2.031 Å in TS1 and further to 1.535 Å Int1. This indicates that the C3–O4 bond breaks and C1–C10 bond forms simultaneously. In the intramolecular proton transfer process, the distances of O4–H11 and C10–H11 are 1.386 and 1.431 Å in TS 2-1, respectively, where a four-member ring is formed. Moreover, the bond angle of O4–H11–C10 is 105.7°. In TS2-2, the proton H11 transfers from C10 to O4′ of the second molecule and the proton H11′ transfers from C10′ of the second molecule to O4 in a stepwise manner. It is worth noting that the bond angle is 172.1° for ∠C10–H11–O4′ and 160.0° for ∠C10′–H11′–O4. These bond angles are larger than the bond angles in TS 2-1, leading to a smaller ring strain. The results show that intermolecular proton transfer is more feasible than intramolecular counterpart. In TSa3 (pathway A) the O4–H11 bond length is 1.260 Å and C2–H11 bond length is 1.335 Å. It shows that the hydrogen is shared by C2 and O4. Subsequently, isomerization proceeds after [1,5]-sigmatropic reaction, and then the C3–O4 bond length is shortened by about 1.474 Å *via* cyclization forming benzopyran (product A). Pathway B is a dissociation reaction; in allenic phenol, Int 2, deprotonation occurs to form allenic phenolate Intb2. Finally, the last step is cyclization, where O4–C2 bond length is shortened by about 1.418 Å (Intb2 to product B) and forming 2-methylbenzofuran. For pathway C, the cyclization reaction, the O4–C2 bond length is shortened by 1.378 Å (Int2 to IntC3), and undergoes the [1,3]-sigmatropic reaction in which H11 is partially coordinated between C1 and C3 (1.725 and 1.956 Å, respectively) of TSc4 to form 2-methylbenzofuran. In pathway B, one of the steps proceeded through the O–H dissociation. Thus, pK_a [49] is calculated to provide the ability of hydrogen abstraction (see Table S10†). The pK_a results show that the chloro-substituents at the aryl group make the proton abstraction easier and help proceed and facilitate the formation of 2-methyl-benzofuran.

3.2. Potential energy surface and reaction mechanism

The relative potential energy surface for aryl propargyl ether Claisen rearrangement in the gas and *N*,*N*-diethylaniline phase is shown in Fig. 2 and detailed information is given in Table 1. The plausible mechanism for aryl propargyl ether Claisen rearrangement is known to be pericyclic. The pericyclic reaction pathway can be observed from TS1, TS2-1 and TS2-2. As shown in Table 1, it can be observed that the difference between Gibbs free energy of the gas-phase and the solvent phase is larger because Intb2, TSb3 and product B complex have ionic species. The variations for other TS and Int in the gas-phase and the solvent phase are not too large (about

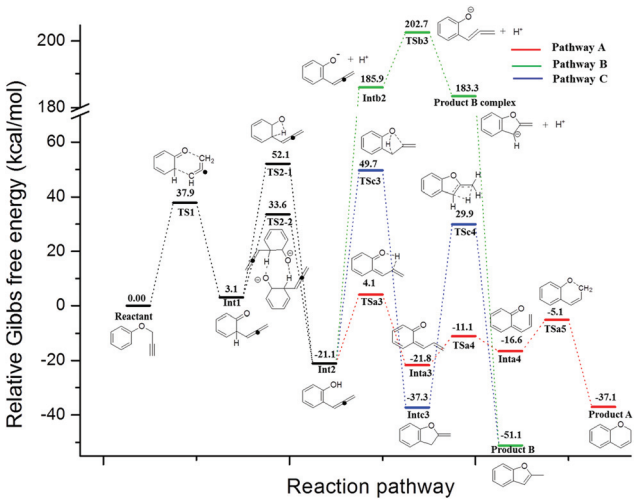

Fig. 2 Computed potential energy surface for aryl propargyl ether Claisen rearrangement in the solvent phase at M06/6-31+G**//B3LYP/6-31+G* level of theory.

0.8 kcal mol^{-1}). Therefore, the following discussion is based on solvent phase results. Also, experimental reactions were carried out using *N*,*N*-diethylaniline as a solvent.

As seen from Fig. 2, for TS1 in the solvent phase, the energy barrier of C3–O4 bond breaking and C1–C10 bond forming is 37.9 kcal mol^{-1} with loss of aromaticity. The intramolecular (TS2-1) and intermolecular (TS2-2) proton transfer occurs with an energy barrier of 52.1 and 33.6 kcal mol^{-1}, respectively. The lowest energy barrier of intermolecular proton transfer is energetically more favorable than intramolecular proton transfer. Three different pathways were followed from the allenic phenol intermediate (Int2). For pathway A, the energy barrier is 25.2 kcal mol^{-1} for [1,5]-sigmatropic reaction and 11.5 kcal mol^{-1} for cyclization. Meanwhile, isomerization requires overcoming the energy barrier of 10.7 kcal mol^{-1}. Isomerization takes place from s-*trans* conformation (Inta3) to s-*cis* conformation (Inta4) and finally yields benzopyran (Product A). The energy barrier has decreased chronologically from In2 to Product A, in pathway A, owing to the extended conjugation cycle and finally ends up with the oxa-Diels–Alder reaction to form benzopyran. Overall, the reaction in pathway A has to be considered as a concerted reaction. For pathway B, the dissociation energy (D_e) of Intb2 is too high, about 207 kcal mol^{-1}. Cyclization from allenic phenolate, Intb 2, to form product B complex *via* TSb3 requires an energy barrier of 16.8 kcal mol^{-1}. Further, the abstraction of H^+ yields 2-methylbenzofuran, exothermic, with large formation energy. pK_a was calculated for O–H dissociation in allenic phenol (Int2). The pK_a calculations were performed at M06/6-31+G**//B3LYP/6-31+G* in the gas and solvent phase which included both thermodynamic cycles. The pK_a values are listed in Table S10.† The acidic nature of allenic phenol can be observed from the value of pK_a. The acidity of allenic phenol (Int2) is quite higher as compared to phenol.[50] The value of pK_a has increased while increasing the number of methyl groups at C3

position, due to the steric hindrance near the –OH group. The pK_a cycle and results clearly suggest that strong base is required to obtain the benzofuran product (product B) experimentally. Also, substitution of the methyl and methoxy groups has increased the pK_a value while chloro substitution has decreased the pK_a along with the methyl groups at C3 position due to the inductive effect. In pathway C, allenic phenol (Int2) precedes cyclization *via* 70.8 kcal mol^{-1} energy barrier, and follows [1,3]-sigmatropic rearrangement which requires an energy of 67.2 kcal mol^{-1} to form 2-methylbenzofuran. The energy barrier of pathway C is higher and it was not discussed further.

TS1, TS2-1 and TS2-2 may be considered as pericyclic reactions, due to their higher energy barrier than the rest of the successive pathways. From Int2 onwards the mechanism has followed three different plausible pathways to yield benzofuran and benzopyran moieties. In pathway A, the TSa3 and TSa4 barrier energy is lower as compared with TS1 and TS2-2. In TSa3 the phenolic bond is broken with one orbital disconnection at the oxygen. Also, in TSa5 an ether bond is forming through oxa-Diels–Alder reaction. Overall, the pericyclic reactions (TS1, TS2-2) are followed by bond breaking and bond forming reactions with a low barrier energy due to extended conjugation in TSa3 and TSa5.

From Fig. 2 and Table 1, the energy barrier of [3,3]-sigmatropic reaction is 37.9 kcal mol^{-1} for TS1. The energy barrier for the O4–C10 bond breaking and C1–C10 bond formation are key steps in aryl propargyl ether Claisen rearrangement. From the energy barrier, it can be concluded that the [3,3]-sigmatropic reaction is the rate-limiting step for the pathway A and pathway B. In summary, pathways A and B are more favorable for benzopyran and 2-methyl-benzofuran, respectively, in the overall mechanism.

From the thermodynamic properties, Gibbs free energies of the final products benzopyran and 2-methyl-benzofuran are −37.1 and −51.1 kcal mol^{-1} in the solvent phase, respectively. It is worth noting that only the energy of allenic dienone, Int 1, related to the reactant is positive owing to the loss of its aromaticity. The first step is the rate-determining step and its energy barrier is 37.9 kcal mol^{-1}, and the following barrier of the reaction is lower. Moreover, the energy barrier for TSa4 is 10.7 kcal mol^{-1} which is simple isomerization of *-trans* to *-cis* conformation. In pathway A, exocyclic extended conjugation plays a crucial role for the low energy barrier. Therefore, once beyond the rate-determining step, the next step has enough energy to precede the reaction quickly. The formation of 2-methyl-benzofuran is more exothermic than benzopyran formation, that is, 2-methyl-benzofuran is more stable than benzopyran.

3.3. Substituent effects

In order to understand the substituent effects on the kinetics of aryl propargyl ether Claisen rearrangement, substitutions on the aryl and aliphatic segments are considered. Scheme 2 represents possible substitution sites on aryl propargyl ether. Methyl, methoxy and chloro groups have been considered substitution groups at *ortho*-, *meta*- and *para*-positions in the aromatic ring for the study. The *meta*-substitution has two possible reaction orientations and gives a mixture of *ortho*- and *para*-cyclized products.

Tables 4–6 presents the energy barrier for the first two steps of bond breaking and new bond forming reactions for the

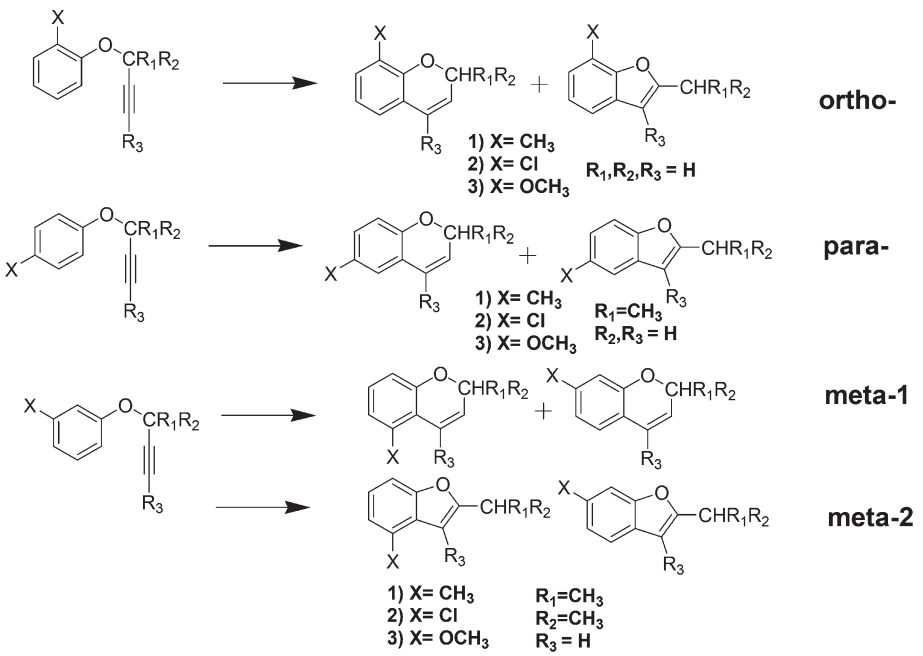

Scheme 2 Various possible substitutions at the aryl and C3 position of the alkyl group.

Table 4 Energy barrier of the first two steps of the methyl group on the aromatic segment with zero, mono and dimethyl groups on the aliphatic segment in *N*,*N*-diethylaniline at M06/6-31+G**//B3LYP/6-31+G* level[a]

	Parent	1a-*o*	1a-*p*	1a-*m*1	1a-*m*2	1b-*o*	1b-*p*	1b-*m*1	1b-*m*2	1c-*o*	1c-*p*	1c-*m*1	1c-*m*2
Step 1	37.9	37.0	38.2	37.7	36.7	35.3	36.7	36.1	35.5	29.9	31.4	31.9	30.3
Step 2	30.6	30.1	30.9	28.4	29.4	31.3	33.2	30.9	31.7	31.2	33.8	31.1	30.0

[a] *ortho*- is denoted by *o*-; *para*- is denoted by *p*-; *meta*-1 is denoted by *m*1; *meta*-2 is denoted by *m*2. a, b and c represents the zero, mono and dimethyl group on the aliphatic segment, respectively.

Table 5 Energy barrier of the first two steps of chloro group on aromatic segment with zero, mono and dimethyl groups on the aliphatic segment in *N*,*N*-diethylaniline at M06/6-31+G**//B3LYP/6-31+G* level[a]

	Parent	2a-*o*	2a-*p*	2a-*m*1	2a-*m*2	2b-*o*	2b-*p*	2b-*m*1	2b-*m*2	2c-*o*	2c-*p*	2c-*m*1	2c-*m*2
Step 1	37.9	36.4	38.1	37.7	36.7	34.2	36.0	35.8	34.8	29.0	30.6	30.2	29.4
Step 2	30.6	30.3	31.5	29.7	31.1	31.5	32.9	30.3	32.1	31.9	33.7	30.1	32.9

[a] *ortho*- is denoted by *o*-; *para*- is denoted by *p*-; *meta*-1 is denoted by *m*1; *meta*-2 is denoted by *m*2. a, b and c represents the zero, mono and dimethyl group on the aliphatic segment, respectively.

Table 6 Energy barrier of the first two steps of the methoxy group on aromatic segment with zero, mono and dimethyl groups on the aliphatic segment in *N*,*N*-diethylaniline at M06/6-31+G**//B3LYP/6-31+G* level[a]

	Parent	3a-*o*	3a-*p*	3a-*m*1	3a-*m*2	3b-*o*	3b-*p*	3b-*m*1	3b-*m*2	3c-*o*	3c-*p*	3c-*m*1	3c-*m*2
Step 1	37.9	36.1	38.0	35.3	33.6	34.2	36.0	35.6	33.9	29.3	31.0	31.0	29.2
Step 2	30.6	31.8	32.5	27.7	25.9	32.0	34.3	26.4	28.3	32.0	35.5	25.4	27.8

[a] *ortho*- is denoted by *o*-; *para*- is denoted by *p*-; *meta*-1 is denoted by *m*1; *meta*-2 is denoted by *m*2. a, b and c represents the zero, mono and dimethyl group on the aliphatic segment, respectively.

methyl, methoxy and chloro groups on the aromatic and methyl group on the aliphatic segment of the reactant in the solvent phase at M06/6-31+G**//B3LYP/6-31+G* level. The substitution at *meta*-2 position favors the *ortho*-cyclized product due to the lower energy barrier. Moreover, the energy barriers are found to be decreasing when the number of methyl groups at C3 position has increased for the above mentioned three different functional groups on the aromatic ring. From the results, it can be concluded that the methyl, methoxy and chloro groups at *o*, *m*, and *p* positions on the aromatic segment decrease the energy barrier slightly and the methyl groups at C3 position have reduced the energy barrier greatly. However, these substituents do not affect remarkably the tautomerization of the reaction. Therefore step 2, the proton transfer reaction, becomes the rate-determining-step.

Besides, the C3–O4 and O4–C5 bond can rotate freely for the aryl propargyl ether and produce different conformational isomers. Fig. 3 shows the geometric structures for the two lowest energy conformational isomers. As seen in Fig. 3, when the number of methyl groups increases, the energy difference becomes larger from 0.6 to 2.1 kcal mol^{-1}. Therefore, the substitution of more methyl groups at C3 position is found to be a better orientation for the reactant to facilitate the aryl propargyl ether Claisen rearrangement.

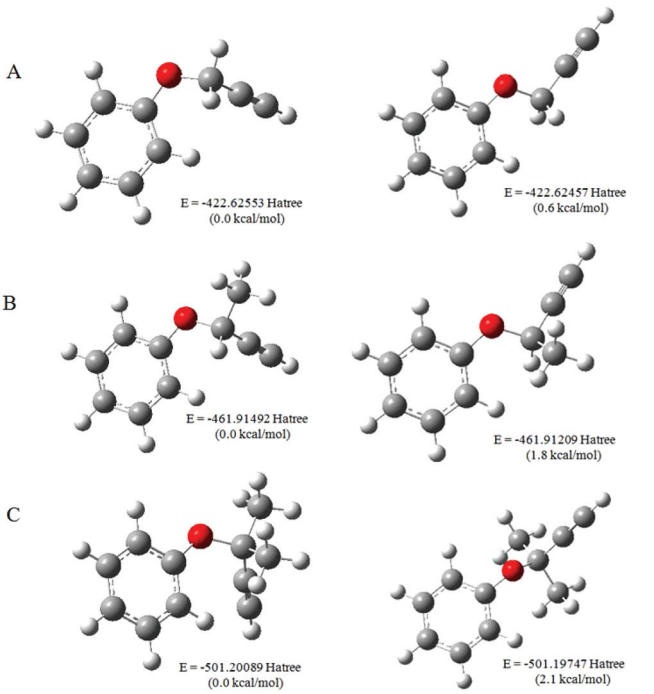

Fig. 3 Geometries and the relative energies of the reactant for different conformational isomerisms in the gas phase at M06/6-31+G**//B3LYP/6-31+G* level.

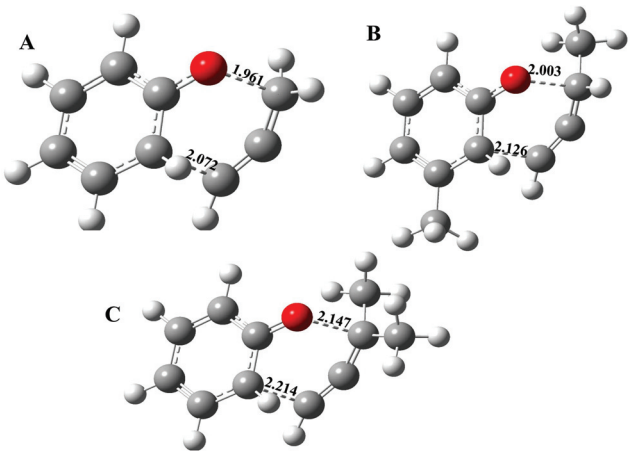

Fig. 4 Three geometries of transition structures are chosen for NBO analysis to explore the substituent effect of the methyl group at C3-position. The bond distances are in Å.

Table 7 Selected donor–acceptor bond orbital interaction and ΔE_2 values (kcal mol^{-1}) for transition state species (geometries in Fig. 4) of aryl propargyl ether Claisen rearrangement[a]

Species	Donor	Acceptor	Interaction	$E(2)$
A	BD C1–C10	BD* C5–O4	$\sigma \rightarrow \pi^*$	27.25
	BD C1–C10	BD* C2–C3	$\sigma \rightarrow \pi^*$	18.8
	BD C5–O4	BD* C2–C3	$\pi \rightarrow \pi^*$	25.33
	BD* C5–O4	BD* C2–C3	$\pi^* \rightarrow \pi^*$	85.7
B	BD C1–C10	BD* C5–O4	$\sigma \rightarrow \pi^*$	30.89
	BD C1–C10	BD* C2–C3	$\sigma \rightarrow \pi^*$	20.93
	BD C5–O4	BD* C2–C3	$\pi \rightarrow \pi^*$	15.08
	BD* C5–O4	BD* C2–C3	$\pi^* \rightarrow \pi^*$	74.29
C	BD C1–C10	BD* C5–O4	$\sigma \rightarrow \pi^*$	33.24
	BD C1–C10	BD* C2–C3	$\sigma \rightarrow \pi^*$	22.16
	BD C5–O4	BD* C2–C3	$\pi \rightarrow \pi^*$	9.99
	BD* C5–O4	BD* C2–C3	$\pi^* \rightarrow \pi^*$	61.32

[a] NBO analysis is performed at the M06/6-31+G**//B3LYP/6-31+G* level. BD and BD* denote the occupied bond and formally empty antibonding orbital, respectively.

NBO analyses[45,46] have also been performed to rationalize the aforementioned results by increasing the number of methyl groups at C3 position, which facilitates the aryl propargyl ether Claisen rearrangement. NBO analysis is carried out for the transition state structures of A, B and C shown in Fig. 4. Donor–acceptor stabilization energies from NBO analysis for these three transition state structures are collected and listed in Table 7. As can be seen in Table 7, for each transition state structure, the donor–acceptor interaction involves $\pi \rightarrow \pi^*$ and $\pi^* \rightarrow \pi^*$ between C5–O4 and C2–C3, the $\sigma \rightarrow \pi^*$ between C1–C10 and C5–O4, and the $\sigma \rightarrow \pi^*$ between C1–C10 and C2–O3 contribute to their stabilization energy. The total stabilization energies are 157.08, 141.19, 126.71 kcal mol^{-1} for the transition state structures of A, B and C, respectively. Larger stabilization energy results with a higher energy barrier in step 1 have blocked the aryl propargyl ether Claisen rearrangement. In other words, methyl group substitution at C3 position has revealed the smaller stabilization energy and thus decreases the energy barrier, which helps facilitate the aryl propargyl ether Claisen rearrangement.

4. Conclusions

Three possible pathways for aryl propargyl ether Claisen rearrangement were investigated. The pathway A and pathway B are the most possible routes to form benzopyran and benzofuran, respectively. The rate-limiting step is the first step in aryl propargyl ether Claisen rearrangement with $\Delta G^{\ddagger}$ being 38.4 and 37.9 kcal mol^{-1} in the gas and solvent phase, respectively, for the parent aryl propargyl ether. Different DFT methods are performed to check the energy barrier and the results at M06/6-31+G**//B3LYP/6-31+G* level are in good agreement with the experimental values. At this level, the MUE and RMSE values are 1.0 and 1.4 kcal mol^{-1}, respectively. For the substituent effects, one can find the energy barrier for the substituent in the *para*-position is higher than those in *ortho*- and *meta*-positions. The substitution of methyl groups at C3 position leads to decreasing the energy barrier dramatically and changing the rate-limiting step from the [3,3]-sigmatropic reaction to a proton transfer step. According to the results of structural information, the substitution of methyl groups at C3 position makes the C3–O4 bond lengthen from 1.43 to 1.45 Å and the C1–C10 bond to shorten from 3.97 to 3.70 Å in the reaction center of aryl propargyl ether. In addition, the methyl groups at C3 position might lead to the correct orientation for the reaction to proceed. Also, the donor–acceptor NBO results suggest that the methyl group substitution at C3 position helps to precede the aryl propargyl ether Claisen rearrangement reaction smoothly.

Acknowledgements

This research was supported by the National Science Council (NSC) of Taiwan, and the computational resource was partially supported by the National Center for High-Performance Computing (NCHC), Hsin-Chu, Taiwan. We also gratefully acknowledge Dr Yu-Wei Huang for his valuable assistance and discussion at the time of work.

References

1 A. M. M. Castro, *Chem. Rev.*, 2004, **104**, 2939.
2 L. Claisen, *Ber. Dtsch. Chem. Ges.*, 1912, **45**, 3157.
3 I. Iwai and J. Ide, *Chem. Pharm. Bull.*, 1962, **10**, 926.
4 J. Zsindely and H. Schmidt, *Helv. Chim. Acta*, 1968, **51**, 1510.
5 I. Iwai and J. Ide, *Chem. Pharm. Bull.*, 1963, **11**, 1042.
6 J. Hlubucek, E. Ritchie and W. C. Taylor, *Aust. J. Chem.*, 1971, **24**, 2347.

7 M. Harfenist and E. Thom, *J. Org. Chem.*, 1972, **37**, 841.
8 W. K. Anderson and E. J. Lavoie, *J. Org. Chem.*, 1973, **38**, 3832.
9 W. K. Anderson, E. J. Lavoie and P. G. Whitkop, *J. Org. Chem.*, 1974, **39**, 881.
10 H. Ishii, T. Ishikawa, S. Takeda, S. Ueki and M. Suzuki, *Chem. Pharm. Bull.*, 1992, **40**, 1148.
11 S. J. Pastine, S. W. Youn and D. Sames, *Tetrahedron*, 2003, **59**, 8859.
12 V. V. V. N. S. R. Rao, G. V. Reddy, R. Yadla, B. Narsaiah and P. S. Rao, *ARKIVOC*, 2005, **iii**, 211.
13 S. A. Worlikar, T. Kesharwani, T. Yao and R. C. Larock, *J. Org. Chem.*, 2007, **72**, 1347.
14 R. S. Kenny, U. C. Mashelkar, D. M. Rane and D. K. Bezawada, *Tetrahedron*, 2006, **62**, 9280.
15 F. A. Khan and L. Soma, *Tetrahedron Lett.*, 2007, **48**, 85.
16 B. Lu, B. Wang, Y. Zhang and D. Ma, *J. Org. Chem.*, 2007, **72**, 5337.
17 A. K. Yadav, B. K. Singh, N. Singh and R. P. Tripathi, *Tetrahedron Lett.*, 2007, **48**, 6628.
18 N. R. Curtis, J. C. Prodger, G. Rassias and A. J. Walker, *Tetrahedron Lett.*, 2008, **49**, 6279.
19 V. S. P. R. Lingam, R. Vinodkumar, K. Mukkanti, A. Thomas and B. Gopala, *Tetrahedron Lett.*, 2008, **49**, 4260.
20 B. Godoi, A. Sperança, D. F. Back, R. Brandão, C. W. Nogueira and G. Zeni, *J. Org. Chem.*, 2009, **74**, 3469.
21 R. S. Menon, A. D. Findlay, A. C. Bissember and M. G. Banwell, *J. Org. Chem.*, 2009, **74**, 8901.
22 I. N. Lykakis, C. Efe, C. Gryparis and M. Stratakis, *Eur. J. Org. Chem.*, 2011, 2334.
23 C. L. Chung, C. H. Han, H. M. Wang, R. S. Hou and L. C. Chen, *J. Chin. Chem. Soc.*, 2001, **58**, 90.
24 N. Majumdar, K. A. Korthals and W. D. Wulff, *J. Am. Chem. Soc.*, 2012, **134**, 1357.
25 M. S. Dewar and E. F. Healy, *J. Am. Chem. Soc.*, 1984, **106**, 7127.
26 M. M. Khaledy, M. Y. S. Kalani, K. S. Khuong and K. N. Houk, *J. Org. Chem.*, 2003, **68**, 572.
27 S. Gül, F. Schoenebeck, V. Aviyente and K. N. Houk, *J. Org. Chem.*, 2010, **75**, 2115.
28 J. Rehbein, S. Leick and M. Hiersemann, *J. Org. Chem.*, 2009, **74**, 1531.
29 O. Acevedo and K. Armacost, *J. Am. Chem. Soc.*, 2010, **132**, 1966.
30 Y. Zheng and J. Zhang, *J. Phys. Chem. A*, 2010, **114**, 4325.
31 A. D. Becke, *Phys. Rev. A: At., Mol., Opt. Phys.*, 1988, **38**, 3098.
32 A. D. Becke, *J. Chem. Phys.*, 1993, **98**, 5648.
33 A. D. Becke, *J. Chem. Phys.*, 1997, **107**, 8554.
34 C. Lee, W. Yang and R. G. Parr, *Phys. Rev. B: Condens. Matter*, 1988, **37**, 785.
35 H. L. Schmider and A. D. Becke, *J. Chem. Phys.*, 1998, **108**, 9624.
36 Y. Zhao and D. G. Truhlar, *Theor. Chem. Acc.*, 2008, **120**, 215.
37 Y. Zhao, N. E. Schultz and D. G. Truhlar, *J. Chem. Theory Comput.*, 2006, **2**, 364.
38 J. P. Moreno and M. G. Kuzyk, *J. Chem. Phys.*, 2005, **123**, 194101.
39 J. D. Chai and M. Head-Gordon, *Phys. Chem. Chem. Phys.*, 2008, **10**, 6615.
40 A. D. Boese and J. M. L. Martin, *J. Chem. Phys.*, 2004, **121**, 3405.
41 S. Grimme, *J. Chem. Phys.*, 2006, **124**, 034108.
42 J. Tomasi and M. Persico, *Chem. Rev.*, 1994, **94**, 2027.
43 J. Tomasi, B. Mennucci and R. Cammi, *Chem. Rev.*, 2005, **105**, 2999.
44 M. J. Frisch, G. W. Trucks, H. B. Schlegel, G. E. Scuseria, M. A. Robb, J. R. Cheeseman, G. Scalmani, V. Barone, B. Mennucci and G. A. Petersson, *et al.*, *GAUSSIAN 09, (Revision A.1)*, Gaussian, Inc., Wallingford, CT, 2009.
45 E. D. Glendening, A. E. Reed, J. E. Carpenter and F. Weinhold, *NBO 3.0 Program Manual*.
46 E. D. Glendening, C. R. Landis and E. Weinhold, *Wiley Interdiscip. Rev.: Comput. Mol. Sci.*, 2012, **2**, 1.
47 T. R. Ramadhar and R. A. Batey, *Comput. Theor. Chem.*, 2011, **976**, 167.
48 S. Yamabe, S. Okumoto and T. Hayashi, *J. Org. Chem.*, 1996, **61**, 6218.
49 J. Ho and M. L. Coote, *Theor. Chem. Acc.*, 2010, **125**, 3.
50 M. D. Liptak, K. C. Gross, P. G. Seybold, S. Feldgus and G. C. Shields, *J. Am. Chem. Soc.*, 2002, **124**, 6421.